Large Molecule Therapeutics Discovery & Preclinical Development

Molecular Cancer Therapeutics

A Recombinant Immunotoxin against the Tumor-Associated Antigen Mesothelin Reengineered for High Activity, Low Off-Target Toxicity, and Reduced Antigenicity

John E. Weldon, Laiman Xiang, Jingli Zhang, Richard Beers, Dawn A. Walker, Masanori Onda, Raffit Hassan, and Ira Pastan

Abstract

SS1P is a recombinant immunotoxin (RIT) engineered for the targeted elimination of malignant cells that express the tumor-associated antigen mesothelin. It is composed of an antimesothelin antibody variable fragment (Fv) linked to a cytotoxic fragment of *Pseudomonas* exotoxin A (PE) that includes domains II and III of native PE. The clinical use of SS1P is limited by its propensity to induce neutralizing antibodies and to cause a dose-limiting capillary leak syndrome (CLS) in patients. In this article, we describe a reengineered SS1P with improved properties that overcome these deficits. The redesign of SS1P consists of (i) removing the bulk of PE domain II (residues 251–273 and 284–394 of native PE), leaving only an 11-residue furin cleavage site, (ii) adding a Gly–Gly–Ser peptide linker after the furin cleavage site, and (iii) replacing eight highly solvent-exposed residues in the catalytic domain of PE. The new molecule, SS1-LR/GGS/8M, has cytotoxic activity comparable with SS1P on several mesothelin-expressing cell lines and remarkably improved activity on primary cells from patients with mesothelioma. In a mouse xenograft tumor model, high doses of SS1-LR/GGS/8M elicit antitumor activity superior to the activity of SS1P at its maximum-tolerated dose. In addition, SS1-LR/GGS/8M has greatly decreased ability to cause CLS in a rat model and reduced antigenicity or reactivity with antibodies to the sera of patients previously treated with SS1P. *Mol Cancer Ther; 12(1); 48–57.* ©*2012 AACR.*

Introduction

Recombinant immunotoxins (RIT) are engineered therapeutic proteins that combine an antibody fragment with a cytotoxic protein, typically derived from a bacterial or plant source. RITs are designed to serve as selective cytotoxic agents for the targeted elimination of cells with high specificity and high activity and without the secondary toxicities associated with chemotherapy. We have constructed RITs for the treatment of cancers by fusing the antibody variable fragment (Fv) of antibodies against tumor-associated cell surface antigens to a fragment of *Pseudomonas* exotoxin A (PE). RITs using a 38-kDa truncation of PE (PE38) have met with success in clinical trials, especially for the treatment of hematologic malignancies (1–4), such as drug-resistant hairy cell leukemia, in which malignant cells are readily accessible and patients can often be given many cycles of treatment before the development of neutralizing antibodies. Clinical trials to treat solid tumors (5–9) such as mesothelioma have been promising but less successful due to the early development of neutralizing antibodies and the occurrence of off-target toxicities.

To improve the outcome of treatment with PE-based RITs, we have applied our knowledge of the PE intoxication pathway to the redesign of these proteins. RITs are internalized via receptor-mediated endocytosis and traffic through the endolysosomal system to the Golgi, in which they undergo retrograde transport to the endoplasmic reticulum. During this trafficking stage, the toxin is activated through reduction of a disulfide bond and cleavage by the protease furin at a site that separates the Fv from the catalytic fragment of PE. Subsequently, the activated PE must translocate into the cytosol, in which it ADP-ribosylates and inactivates elongation factor 2, an essential component of the translation apparatus. This halts protein synthesis and eventually leads to cell death (for a review see ref. 10). Previous strategies designed to improve the cytotoxic activity of PE-based RITs include substitution of the native C-terminal residues of PE, REDLK, with the canonical endoplasmic reticulum–retention signal KDEL (11–14). This substitution is known to

Authors' Affiliation: Laboratory of Molecular Biology, Center for Cancer Research, National Cancer Institute, NIH, Bethesda, Maryland

Note: Supplementary data for this article are available at Molecular Cancer Therapeutics Online (http://mct.aacrjournals.org/).

Current Address for John E. Weldon: Department of Biological Sciences, Towson University, Towson, MD.

Corresponding Author: Ira Pastan, Laboratory of Molecular Biology, National Cancer Institute, 37 Convent Drive, Room 5106, Bethesda, MD 20892. Phone: 301-496-4797; Fax: 301-402-1344; E-mail: pastani@mail.nih.gov

doi: 10.1158/1535-7163.MCT-12-0336

enhance the cytotoxicity of PE, presumably by improving the efficiency of retrograde transport to the endoplasmic reticulum from the Golgi but can increase off-target toxicity in animal models. Another strategy is to enhance the productive internalization of the RIT-receptor complex, and thereby increase the amount of toxin in the cell by improving the affinity between the Fv and its target (15, 16).

More recently, we have generated a protease-resistant RIT designed to withstand degradation in the endolysosomal system, a potential barrier to effective immunotoxin treatment (17, 18). This lysosomal degradation resistant (LR) variant RIT was produced by removing protease-sensitive regions of PE38, and targeting it to the B-cell specific CD22 receptor with the HA22 high-affinity anti-CD22 Fv (19). We found that the LR mutation did not greatly diminish *in vitro* activity on cell lines, but greatly reduced off-target toxicity in mice and dramatically enhanced activity on patient CLL cells *in vitro*. In addition, the LR variant eliminates 2 major mouse B-cell epitope groups (20) and antigen processing sites from PE38, helping to reduce its immunogenicity in mice (21).

Because of its improved properties in an HA22 background, we chose to adapt the LR variant to SS1P (Fig. 1A), a clinically relevant agent that targets the tumor-associated antigen mesothelin (22). Mesothelin is highly expressed in malignant mesotheliomas, as well as in cancers of the lung, ovary, and pancreas (23). SS1P, which contains the SS1 disulfide-stabilized antimesothelin Fv, is currently undergoing clinical trials for the treatment of mesothelioma (clinicaltrials.gov identifiers NCT01362790 and NCT01445392). Because of the modular nature of RITs, the LR variant of PE should, in principle, be applicable to targeting other tumor-associated antigens by exchanging one Fv for another. The different receptor-mediated pathways by which proteins enter cells, however, are complex and can influence RIT trafficking. CD22, the target of HA22, is expressed exclusively on B cells and associated malignancies, and is a large transmembrane glycoprotein that seems to undergo constitutive clathrin-dependent endocytic recycling (24). In contrast to CD22, mesothelin, the target of SS1P, is a glyocophosphatidylinositol (GPI)-linked protein expressed on epithelial cells. GPI-linked proteins are anchored to the extracellular side of cell membranes by their C-termini, and thus must be internalized and sorted independent of cytosolic interactions (see ref. 25 for a review). Differences in receptor endocytosis and trafficking could lead to different routes of internalization, and thereby influence the cytotoxic outcome. In addition to the receptor, it is also possible that removing or adding sequences to a RIT could alter its trafficking, processing, and cytotoxic activity.

In this article, we describe the development and properties of a reengineered antimesothelin RIT, SS1-LR/GGS/8M (Fig. 1B and C). SS1-LR/GGS/8M has improved activity on primary cells from patients with mesothelioma, greatly decreased capacity to initiate capillary leak syndrome (CLS) in a rat model, and reduced antigenicity, or reactivity with antibodies in antisera from patients who had previously developed neutralizing antibodies against SS1P. On the basis of these findings SS1-LR/GGS/8M is an excellent candidate for further clinical development.

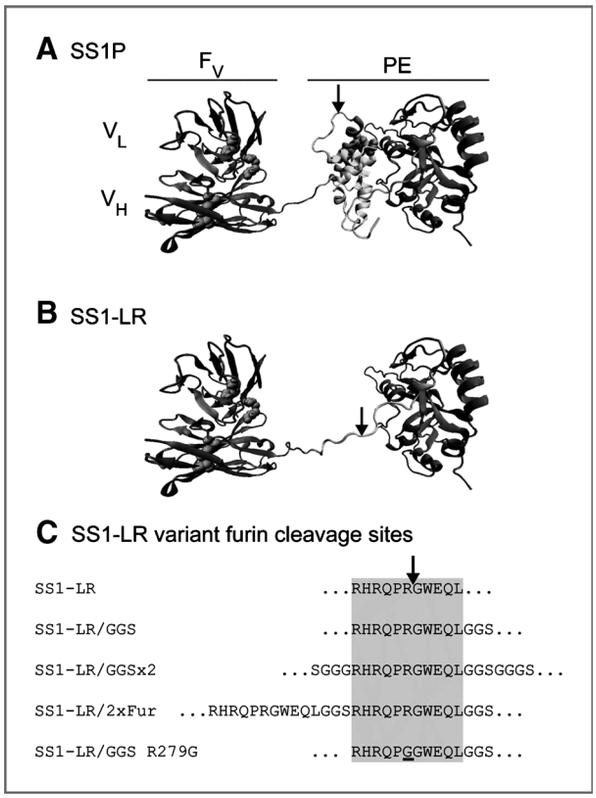

Figure 1. RITs. The RIT SS1P consists of the disulfide-stabilized heavy chain Fv polypeptide (V_H) and light chain Fv polypeptide (V_L) polypeptide chains of the Fv from the antimesothelin monoclonal antibody SS1 coupled to a 38 kDa fragment of PE38. Both the V_H and V_L fragments contain an internal disulfide bond in addition to the interchain disulfide bond engineered between the 2 fragments. A, a structural model of SS1P. The Fv is recombinantly joined to PE38, which is divided into domain II, domain III, and part of domain Ib from native PE38. Disulfide bonds are indicated as space-filling structures. The model contains a gap in the structure that corresponds to the deletion of residues 365 to 380 in domain Ib. B, a model of SS1-LR. SS1-LR lacks the majority of domains Ib and II of PE but includes an 11-residue stretch of domain II that contains the furin cleavage site. Both models are hypothetical arrangements based on the structures of native PE and immunoglobulin G; they do not represent actual structure determinations. C, various constructs were created with mutations around the furin cleavage site of SS1-LR. The furin site from native PE is shaded. Black arrows indicate the position of cleavage between Arg-279 and Gly-280. SS1-LR/GGS R279G contains a point mutation (underlined) that prevents furin cleavage by replacing Arg-279 with Gly.

Materials and Methods

Proteins

SS1P (SS1(dsFv)-PE38) and its derivatives were expressed, refolded, and purified as described (26). SS1P was manufactured by Advanced BioScience Laboratories, Inc. All other RITs were prepared in the Laboratory of

Molecular Biology, National Cancer Institute (NCI; Bethesda, MD). Mutations were generated using Quikchange site-directed mutagenesis (Stratagene) with primers from Lofstrand Labs Limited. Supplementary Fig. S1 shows an SDS-PAGE analysis of the purified proteins.

Cell lines

Several mesothelin-positive human cell lines were used in this study. The L55 lung adenocarcinoma and M30 mesothelioma cell lines were provided by Steven Albelda (University of Pennsylvania, Philadelphia, PA). The HAY mesothelioma cell line was provided by the Stehlin Foundation for Cancer Research (Houston, TX). The OVCAR-8 and A1847 ovarian cancer cell lines were provided by Hisataka Kobayashi and Stuart Aaronson (NCI, Bethesda, MD), respectively. The NCI-H322M lung adenocarcinoma cell line was obtained from the Developmental Therapeutics Program, Division of Cancer Treatment and Diagnosis Tumor Repository (NCI, Frederick, MD). The cell lines A431/K5 (27) and A431/H9 (28) are derivatives of the A431 epidermoid carcinoma cell line that have been stably transfected with vectors for human mesothelin, and grown in media supplemented with 750 μg/mL G-418 (Geneticin) for selection. All cell lines were grown at 37°C with 5% CO_2 in media supplemented with 10% FBS, 2 mmol/L L-glutamine, 100 U penicillin, and 100 μg streptomycin (Invitrogen Corporation). A431/K5 was grown in Dulbecco's modified Eagle's medium; all other lines were grown in RPMI-1640 medium supplemented 1 mmol/L sodium pyruvate (Invitrogen). All cell lines were authenticated at the source and grown from frozen stocks prepared from an early passage of the original line.

Cytotoxicity assays

Viability of cell lines treated with immunotoxins was measured using the Cell Counting Kit-8 WST-8 assay (Dojindo Molecular Technologies, Inc.). Cells (2,000 cells/well) were plated in 96-well plates, left overnight to adhere, and incubated with varying concentrations of RITs for 72 hours at a final volume of 0.2 mL. At the end of the incubation period, 10 μL of the CCK-8 reagent was added to each well and the plates were incubated at 37°C until the wells with the maximum absorbance at 450 nm reached values of approximately 1 optical density (OD). Values were normalized between controls of cyclohexamide (10 μg/mL) and buffer [Dulbecco's PBS without Ca and Mg (D-PBS; Quality Biological, Inc.) containing 0.2% human serum albumin (HSA)], then fit to a sigmoidal equation with variable slopes for the plateau, baseline, and Hill slope using GraphPad PRISM software (GraphPad Software, Inc.). The equation was subsequently used to interpolate the concentration of RIT, which reduced cell viability to the 50% level (EC_{50}).

Primary mesothelioma cell cultures were established as described (29) from the peritoneal or pleural fluid of 4 patients with advanced mesothelioma who were being treated on protocols approved by NCI Institutional Review Board. The resulting cells (NCI-M-02, NCI-M-03, NCI-M-16, and NCI-M-19) were judged by a pathologist to be malignant and subsequently determined to be a single population of mesothelin-expressing cells by flow cytometry. Responses to SS1P and SS1-LR/GGS/8M were evaluated at an early passage using a crystal violet assay. D-PBS and 10 ng/mL HB21 (antitransferrin receptor/PE40) were used as negative and positive controls for cell death, respectively. Each condition was evaluated in triplicate. Statistical analysis of the resulting data by ANOVA was conducted using GraphPad Prism software.

Mouse A431/H9 xenograft antitumor assay

Female nude mice were injected subcutaneously in the flank with 1.8×10^6 A431/H9 cells in 0.2 mL RPMI with 4 mg/mL Matrigel (BD Biosciences) on day 0. Tumor volume was followed by regular caliper measurements. When tumors reached an average size of approximately 110 mm^3, mice were divided into groups and intravenously injected 3 times on days 7, 9, and 12 with 0.2-mL of vehicle (0.2% HSA in D-PBS; $n = 5$) or vehicle containing either SS1P (0.4 mg/kg; $n = 4$) or SS1-LR/GGS/8M (2.5 or 5.0 mg/kg; $n = 6$). Follow-up experiments used the same protocol with 6 doses of 5.0 mg/kg SS1-LR/GGS/8M administered on days 6, 8, 10, 13, 15, and 17 ($n = 10$), and 5 doses of 10.0 mg/kg SS1-LR/GGS/8M administered on days 6, 8, 10, 17, and 20 ($n = 8$). This experiment and all subsequent animal experiments were handled according to the NIH guidelines approved by the Animal Care and Use Committee of the NCI.

Mouse serum pharmacokinetics

Groups of 9 female nude mice were injected intravenously with 10 μg of SS1P or SS1-LR/GGS/8M in 0.2 mL of 0.2% HSA in D-PBS. Subgroups of 3 mice were bled at time intervals of 2 and 20, 5 and 30, or 10 and 60 minutes. Sera were analyzed by ELISA as previously described (30).

Rat capillary leak assay

A previously described rat model of RIT-induced CLS (31) was used to evaluate the off-target toxicity of SS1-LR/GGS/8M. Briefly, 6- to 8-week-old female Wistar Furthand Rowett, nu/nu (athymic) rats (Harlan-Sprague-Dawley) were injected intravenously with D-PBS, SS1P (0.2 or 0.3 mg/kg), or SS1-LR/GGS/8M (6 or 12 mg/kg). After 24 hours, the rats were euthanized and hydrothorax fluid was collected from the animals. The lungs from several rats were removed, fixed for 3 days in 10% formalin, sectioned, and stained.

Antigenicity assay

Binding of SS1P or SS1-LR/GGS/8M to antibodies in patient sera was analyzed essentially as described (32), except that CD22-rFc and HA22 were used for the detection of PE-specific antibodies by ELISA. Human sera were obtained under protocols 01-C-0011, 03-C-0243, and 08-C-0026.

Results and Discussion

SS1-LR

The immunotoxin SS1P (Fig. 1A) is composed of the disulfide-stabilized 2-chain antimesothelin SS1 Fv joined to PE38 (27, 33, 34). It has high cytotoxic activity on many cancer cell lines that express mesothelin, and has shown partial responses in clinical trials (5–7). The therapeutic potential of SS1P, however, is limited by its immunogenicity and its off-target toxicity. A recently designed variant of PE38, called LR (19; PE Δ251–273 and Δ285–394), has produced lower immunogenicity and off-target toxicity in mice, and could potentially alleviate these deficits in SS1P. We generated SS1-LR (Fig. 1B and C) by replacing the Fv of HA22-LR (19) with the SS1 Fv, and tested it against a panel of 8 cell lines that express mesothelin (Fig. 2). Unexpectedly, SS1-LR was considerably less active than SS1P. One of the mesothelioma cell lines, HAY, showed enhanced sensitivity to SS1-LR, but all of the other cell lines were more resistant. The ovarian cancer cell lines A1847 and OVCAR-8 were particularly resistant to SS1-LR. A complete assessment of the EC_{50} values can be found in Supplementary Table S1, and representative individual cytotoxicity assays are shown in Supplementary Fig. S2.

In native PE and PE38 RITs, the furin cleavage site is presented in a fixed orientation on a highly solvent exposed loop that is stabilized by a disulfide bond (Fig. 1A; ref. 35). Presumably, this conformation enhances the accessibility of the furin site for efficient cleavage by the membrane-bound furin protease. In contrast, the furin cleavage site of SS1-LR is a short tether between 2 larger protein domains, the SS1 Fv and the catalytic domain of PE, which could limit the conformational accessibility of the furin site. This does not seem to be a problem for HA22-LR internalized through CD22, but the internalization pathway of SS1-LR through mesothelin, which does not follow the typical clathrin-dependent mechanism (25), might restrict access to furin. Furin is a transmembrane protein with an extracellular/lumenal protease domain that follows a cell surface to Golgi recycling pathway (36). Both steric accessibility and the trafficking pathway could limit the essential furin cleavage step and reduce the cytotoxicity of SS1-LR.

SS1-LR/GGS

We designed several mutants to explore whether improving the accessibility of the furin cleavage site could enhance the activity of SS1-LR. Our strategy was to increase the length and flexibility of the furin site by the addition of Gly–Gly–Ser linkers. The RIT SS1-LR/GGS (Fig. 1B and C) includes a Gly–Gly–Ser linker on the C-terminal end of the 11-residue furin cleavage site, and has enhanced activity relative to SS1-LR on all cell lines tested (Fig. 2 and Supplementary Table S1). Sample cytotoxicity curves are included in Supplementary Fig. S2. Neither increasing the length of the linker (SS1-LR/GGSx2; Fig. 1B and C) nor duplication of the furin cleavage site with additional linker regions (SS1-LR/2xFur; Fig. 1B and C) enhanced the cytotoxicity beyond that of SS1-LR/GGS (data not shown). Thus, by appending a flexible linker to the SS1-LR furin site, we produced a more active RIT.

To confirm the importance of furin cleavage in the intoxication process, we also prepared the mutant SS1-LR/GGS R279G (Fig. 1B and C), which includes a point mutation of Arg to Gly at the site of hydrolysis that prevents furin cleavage. This mutant showed greatly reduced activity on the 6 cell lines tested, with negligible effect at concentrations up to 1 μg/mL (Supplementary

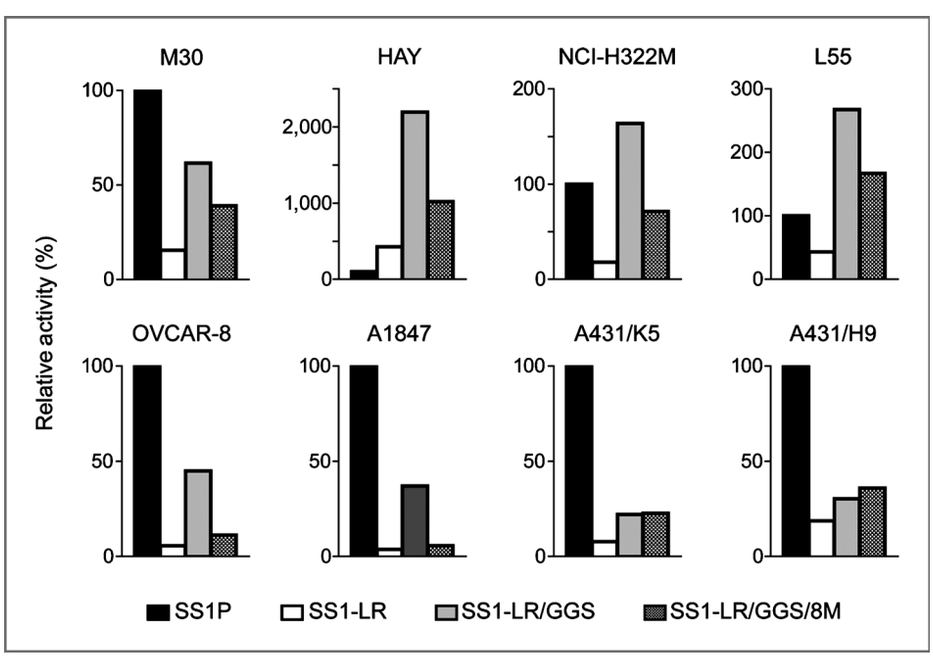

Figure 2. Relative cytotoxicity *in vitro*. A panel of 8 cell lines that express mesothelin was used to compare the cytotoxicities of SS1P, SS1-LR, SS1-LR/GGS, and SS1-LR/GGS/8M. For each cell line, the average EC_{50} of each RIT relative to the average EC_{50} of SS1P is presented.

Table S1). This shows that furin cleavage is essential for the full cytotoxicity of SS1-LR/GGS. The necessity of furin cleavage in the PE intoxication pathway has recently been questioned (37), but much evidence exists that furin cleavage is an important step during the PE intoxication pathway (e.g., refs. 38–40, see ref. 10 for further discussion). In the data presented here, PE intoxication is extraordinarily inefficient without a furin-processing site. Experiments are ongoing to more fully explore the role of furin cleavage in RIT intoxication.

SS1-LR/GGS/8M

Immunogenicity is a particular problem for SS1P in the treatment of patients with intact immune systems (discussed further in ref. 10). Previous research has identified 8-point mutations in domain III (D406A, R432G, R467A, R490A, R513A, E548S, Q592A, and K590S) that silence B-cell epitopes and dramatically reduce the immunogenicity of PE38 RITs in mice (32). We engineered SS1-LR/GGS to include these mutations, generating a new variant called SS1-LR/GGS/8M, and tested it against our panel of mesothelin-expressing cell lines (Fig. 2). The EC_{50} values from these experiments are reported in Supplementary Table S1. SS1-LR/GGS/8M retains similar activity to SS1P on mesothelioma and lung cancer cell lines and in A431 cells transfected with mesothelin. Compared with SS1P and SS1-LR/GGS, however, the 2 ovarian cancer cell lines were particularly insensitive to SS1-LR/GGS/8M.

Off-target toxicity

RIT off-target toxicity in mice is the result of liver damage, which seems to be caused by sequences in domain II that are absent in LR variant RITs (19, 41). The maximum safe dose of SS1P that can be administered to mice at 3 doses every other day is 0.4 mg/kg. Higher doses cause weight loss and death (Pastan and Xiang, unpublished data). RITs engineered to include the LR variant of PE, however, show greatly reduced off-target toxicity in mice (19). We have administered SS1-LR/GGS/8M to mice in doses up to 10 mg/kg at 3 doses every other day without toxicity (data not shown).

In patients, RITs do not generally produce liver damage. Instead, they may damage capillaries, leading to CLS. This can be a major clinical management problem, because of the constellation of weight gain, edema, and hypotension (for of review of CLS, see ref. 42). It seems likely that the initial peak concentrations of PE-based RITs in the bloodstream can nonspecifically damage the endothelial cells lining the blood vessels (43).

Siegall and colleagues have described a rat model of CLS in which PE induces hydrothorax in rats as a result of damage to the lungs and lung capillaries (31, 44). Because the absence of domain II in LR-based RITs significantly decreases liver toxicity in mice, we reasoned that it might also diminish lung damage in rats. Using the rat CLS model, we administered a single intravenous injection of D-PBS, SS1P, or SS1-LR/GGS/8M and observed the rats for signs of hydrothorax (Fig. 3). Rats intravenously treated with 2 mg/kg SS1P seemed ill after 24 hours, with labored breathing and fluid accumulation in their thoracic cavity. Increasing the dose of SS1P to 3 mg/kg increased the volume of thoracic fluid. In contrast, rats treated with either D-PBS or SS1-LR/GGS/8M (6 and 12 mg/kg) showed no signs of illness and had no fluid in their chest cavity. Lungs from rats treated with D-PBS, SS1P, and SS1-LR/GGS/8M were fixed, sectioned, and stained; those from rats treated with D-PBS or SS1-LR/GGS/8M seemed normal, whereas those from rats treated with SS1P showed signs of toxicity including thickening of the vessels and fluid accumulation in the perivascular spaces (Fig. 3B). We have not yet tested higher doses to determine the precise magnitude of the effect, but there is at least a 6-fold difference in toxicity between SS1P and SS1-LR/GGS/8M using this model. No LR-based RIT has been tested clinically, but this observation strengthens the proposition that the LR-based RITs will have decreased off-target toxicity in patients.

A

Treatment	Dose (mg/kg)	*n*	Condition	Fluid volume (mL)
D-PBS	-	7	Healthy	0
SS1P	2	3	Sick	1.5, 1.5, 0.5
	3	2	Sick	6, 2
SS1-LR/GGS/8M	6	3	Healthy	0
	12	3	Healthy	0

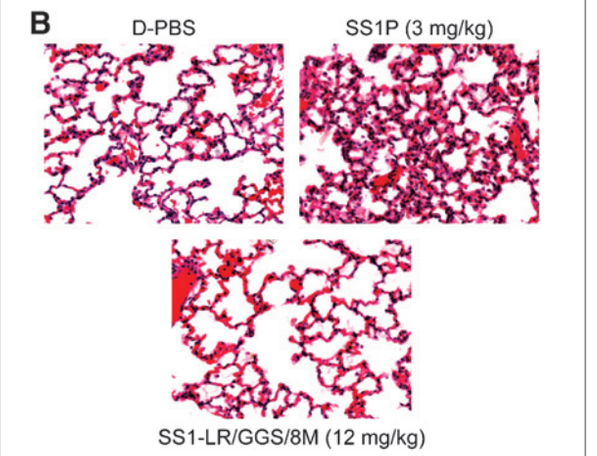

Figure 3. Rat model of CLS. A, rats were grouped and treated intravenously as indicated and evaluated for health before sacrifice after 24 hours. Hydrothorax fluid was removed and measured. B, the lungs of rats from each group were fixed, sectioned, and stained with hematoxylin and eosin. Representative microscopy fields at ×200 magnification are shown.

Mouse A431/H9 tumor model

We evaluated the efficacy of SS1-LR/GGS/8M *in vivo* with a mouse xenograft tumor model using the A431/H9 cell line (Fig. 4). Groups of nude mice ($n = 6$) with tumors averaging 100 to 110 mm^3 were treated intravenously on days 7, 9, and 12 with SS1-LR/GGS/8M at doses of 2.5 and

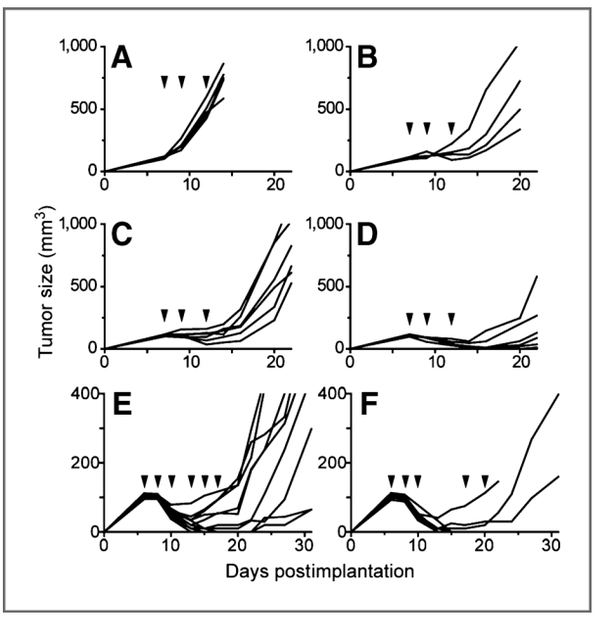

Figure 4. Antitumor activity of SS1-LR/GGS/8M. Nude mice with A431/H9 xenograft tumors were grouped and treated intravenously with SS1-LR/GGS/8M. Initial treatment groups consisted of vehicle ($n = 5$; A), 0.4 mg/kg SS1P ($n = 4$; B), 2.5 mg/kg SS1-LR/GGS/8M ($n = 6$; C), and 5.0 mg/kg SS1-LR/GGS/8M ($n = 6$; D). Tumor size was measured over the course of 22 days. Experiments were subsequently repeated to evaluate the effect of using a greater number of doses and higher dose levels. These treatment groups consisted of 5.0 mg/kg SS1-LR/GGS/8M ($n = 10$; E) and 10.0 mg/kg SS1-LR/GGS/8M ($n = 8$; F). Tumor size was measured over the course of 31 days. All graphs indicate the tumor sizes of individual mice. Arrowheads indicate days when treatment was administered.

5.0 mg/kg. For comparison, additional groups were treated intravenously on the same schedule with vehicle (0.2% HSA in D-PBS; $n = 5$) or 0.4 mg/kg SS1P ($n = 4$), the maximum-tolerated dose of SS1P under this dosing schedule. The tumor size of each mouse was measured regularly for 22 days postimplantation (Fig. 4A–D).

The tumors of vehicle-treated mice grew to an average size exceeding 400 mm^3 by day 12 postimplantation. The tumors of mice treated with 0.4 mg/kg SS1P showed a brief delay in growth and did not exceed 400 mm^3 in size until past day 16 postimplantation. Because SS1-LR/GGS/8M can be given to mice at high doses without ill effect, we treated mice with 2.5 and 5.0 mg/kg. At a dose of 2.5 mg/kg SS1-LR/GGS/8M, the antitumor effect was slightly better than that of SS1P, but mice receiving a 5.0 mg/kg dose of SS1-LR/GGS/8M showed excellent tumor regression. Tumors reached a minimum average size of approximately 29 mm^3 on day 14, but all tumors had resumed growth by day 22. We conclude from these data that SS1-LR/GGS/8M is less active than SS1P in this model, but can be given at higher doses to achieve a greater antitumor effect.

To assess the potential for a greater number of doses and larger dose levels, we repeated the mouse A431/H9 xenograft tumor assay using 6 doses of 5.0 mg/kg ($n = 10$) and 5 doses of 10.0 mg/kg ($n = 8$) SS1-LR/GGS/8M. The tumor size of each mouse was measured regularly for 31 days postimplantation (Fig. 4E and F). All tumors initially responded to the RIT. One out of the 10 mice in the 6×5.0 mg/kg dose group showed a complete and lasting response, decreasing in size to an undetectable level on day 15 and showing no resumption of growth through the duration of the experiment. The tumors from 2 additional mice decreased in size to undetectable levels (1 observed on day 13 and the other on day 17), but subsequently resumed growth (both observed on day 24). Tumors from the remaining 7 mice decreased to a minimum average size of approximately 39 mm^3 on day 13, but subsequently resumed growth over the remaining duration of the experiment. Tumors from 6 of 7 mice resumed growth before the end of the dose series.

In the final group, 5 of 8 mice given 5 doses of 10 mg/kg SS1-LR/GGS/8M had complete and lasting responses. These mice showed undetectable tumors by day 15 postimplantation, after an initial 3 doses on days 6, 8, and 10, and tumor growth did not resume through day 31. The remaining 3 mice exhibited initial tumor regressions that reached a minimum average size of approximately 20 mm^3 on day 13, but did not respond completely. By day 20, tumors from all 3 of these mice had resumed growth. Additional doses on days 17 and 20 failed to achieve any significant decrease in tumor size. We are currently evaluating tumors from these mice to determine the mechanism of resistance.

Pharmacokinetics

Previous work comparing the half-life of an LR-based RIT to a PE38-based RIT in mice showed that LR had a nearly 2-fold shorter half-life in serum than PE38 (7.8 vs. 14.6 minutes, respectively; 18). The shorter half-life negatively impacts antitumor activity *in vivo* by more rapidly removing the smaller RIT from circulation before it can bind to tumor cells and be internalized. We postulated that this difference was due to increased renal filtration of the smaller molecule, because size is a major determinant of renal filtration (45). Previous studies have shown that the kidney is a major route of the removal of RITs from circulation, probably by glomerular filtration and subsequent metabolism by renal tubular enzymes (46, 47).

We anticipated a difference in half-life between SS1P (63 kDa) and SS1-LR/GGS/8M (50 kDa). SS1P has a molecular weight approaching those of hemoglobin (68 kDa) and serum albumin (69 kDa), proteins that exceed the threshold for glomerular filtration and are poorly filtered from the bloodstream by the kidneys (48). SS1-LR/GGS/8M, however, is significantly smaller and thus more likely to be filtered out of circulation. We treated nude mice intravenously with 10 μg SS1P or SS1-LR/GGS/8M, and analyzed serum samples taken at several time points for the presence of RIT. Mice treated with SS1-LR/GGS/8M showed a half-life of 13 minutes in serum, compared with a half-life of 19 minutes for SS1P

(Supplementary Fig. S3). The half-life of SS1P in patients is much longer, nearly 8 hours at the maximum-tolerated dose (5), but we suspect that the relative half-lives of SS1P and SS1-LR/GGS/8M will be similar between mice and patients.

We have begun work on a strategy to increase the size of SS1-LR/GGS/8M, which may restore a longer half-life. SS1P and SS1-LR/GGS/8M are targeted to mesothelin using the Fv portion of the SS1 antibody, but we have previously reported that RITs constructed with the larger Fab portion of antibodies are also highly active in cell culture (49). We plan to prepare and test SS1 Fab fusions with PE-LR/GGS/8M (73 kDa) to evaluate the proposition that increasing its size will increase the half-life of the molecule. It is possible that these larger molecules may have more difficulty penetrating solid tumors, but we expect them to be very active in combination with chemotherapy, which breaks down barriers to tumor penetration (50).

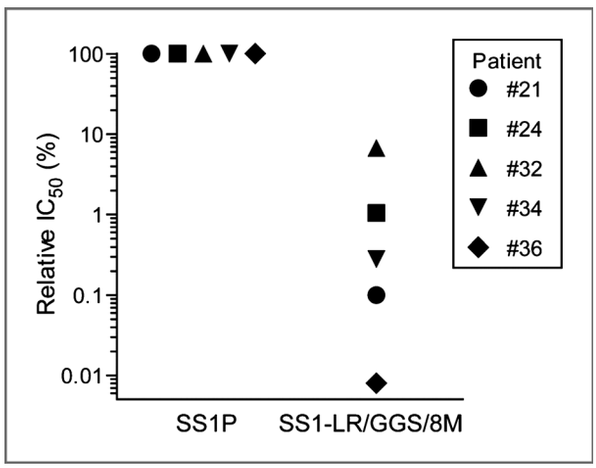

Figure 5. Human antigenicity of SS1-LR/GGS/8M. The reactivity of SS1P and SS1-LR/GGS/8M with preexisting antibodies in human sera was compared using a displacement assay to determine the concentration at which the 2 RITs reduced the signal of an ELISA to detect serum antibodies by 50% (IC_{50}). The IC_{50} values of SS1-LR/GGS/8M relative to SS1P are plotted. Example curves for individual patient sera are provided in Supplementary Fig. S4.

Antigenicity

On the basis of previous research, we assumed that the 8-point mutations in domain III of PE would silence B-cell epitopes, and thereby decrease the immunogenicity of SS1-LR/GGS/8M in mice (32). Because we could not evaluate immunogenicity in humans, however, we instead evaluated the antigenicity of SS1-LR/GGS/8M in human sera from patients who developed neutralizing antibodies to SS1P. Antigenicity refers to the capacity of a molecule to act as a target antigen and react with antibodies.

We obtained serum from 5 patients who had developed neutralizing antibodies in response to treatment with

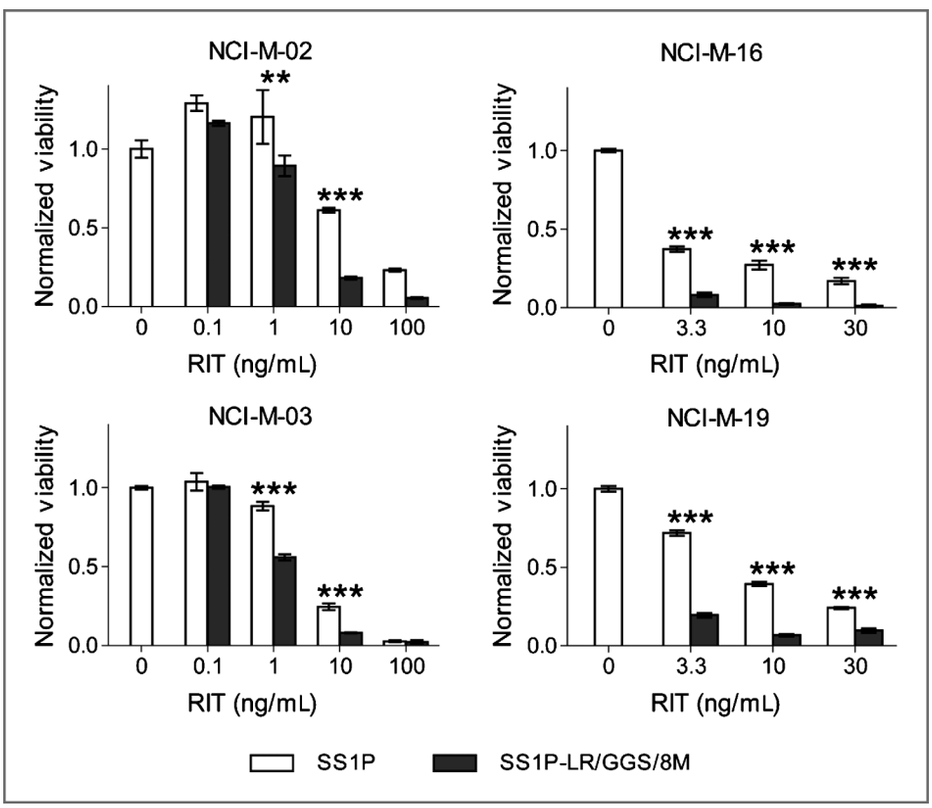

Figure 6. Cytotoxicity of SS1-LR/GGS/8M on patient cells. Cells cultured from the pleural fluid or ascites of patients with mesothelioma were treated with increasing concentrations of SS1P (white bar) or SS1-LR/GGS/8M (gray bar). After 4 days, cells were evaluated for viability using a crystal violet assay. The mean values and SEs from 3 replicates are plotted. Asterisks indicate significant differences of **, $P < 0.01$ or *** $P < 0.001$.

SS1P, and mixed it with dilutions of either SS1P or SS1-LR/GGS/8M to bind reactive antibodies. The remaining unbound complement of PE38-specific antibodies was measured using an ICC-ELISA. From these data, the concentrations of SS1P and SS1-LR/GGS/8M at which the ELISA signal was reduced by 50% (IC_{50}) were determined (example curves are provided in Supplementary Fig. S4). The IC_{50} values correlate with the affinity of the antibody–antigen interaction (20). Figure 5 shows the IC_{50} values of SS1P relative to SS1-LR/GGS/8M plotted as percentages. For all patient sera, the ratios of the IC_{50} values of SS1P relative to SS1-LR/GGS/8M were less than 10%, indicating that the major fraction of SS1P-reactive antibodies in the sera were unreactive with SS1-LR/GGS/8M. This result is consistent with previous observations (32), and indicates that we have identified and silenced the majority of the human immunogenic epitopes in PE38-based RITs. Although SS1-LR/GGS/8M shows reduced antigenicity, an evaluation of its immunogenicity in humans will need to be determined in a clinical trial. Experiments in mice have shown that antigenicity and immunogenicity are closely tied (32), and we anticipate reduced immunogenicity in humans.

Activity on primary patient cells

Because cell line studies do not necessarily predict if new agents will be active in patients, we obtained primary cells from the pleural and peritoneal fluids of patients with mesothelioma and evaluated their sensitivity to SS1-LR/GGS/8M and SS1P after several passages in cell culture (Fig. 6). Viability was assessed 4 days after treatment using a crystal violet assay. The early-passage mesothelioma patient cells NCI-M-02, NCI-M-03, NCI-M-16, and NCI-M-19 showed clear responses to treatment with SS1P (>75% decrease in viability at the 100 ng/mL dose level). The same patient cells showed even greater sensitivity to SS1-LR/GGS/8M. A similarly increased sensitivity was observed when cells derived from patients with chronic lymphocytic leukemia were treated with HA22-LR (19). The mechanism of enhanced sensitivity is not clear, but we hypothesize that LR-based RITs are more stable inside the cell than PE38-based RITs because of decreased susceptibility to degradation.

Concluding remarks

We describe here the development of SS1-LR/GGS/8M, a new and highly active RIT against mesothelin-expressing tumor cells that is a significant improvement over the current clinical molecule, SS1P. Not only does SS1-LR/GGS/8M have high cytotoxic and antitumor activity, but it also can be given safely to rats and mice at doses much higher than SS1P because it does not produce off-target effects. SS1-LR/GGS/8M also has greatly lowered reactivity with human antisera against SS1P, suggesting that it will have decreased immunogenicity in patients. These properties make SS1-LR/GGS/8M a promising candidate for future clinical development.

Disclosure of Potential Conflicts of Interest

M. Onda has ownership interest (including patents). No potential conflicts of interest were disclosed by the other authors.

Authors' Contributions

Conception and design: J.E. Weldon, R. Beers, I. Pastan
Development of methodology: J.E. Weldon, L. Xiang, J. Zhang, R. Beers, D.A. Walker
Acquisition of data (provided animals, acquired and managed patients, provided facilities, etc.): J.E. Weldon, L. Xiang, D.A. Walker, M. Onda, R. Hassan
Analysis and interpretation of data (e.g., statistical analysis, biostatistics, computational analysis): J.E. Weldon, L. Xiang, J. Zhang, R. Beers, M. Onda, I. Pastan
Writing, review, and/or revision of the manuscript: J.E. Weldon, R. Beers, D.A. Walker, M. Onda, R. Hassan, I. Pastan
Administrative, technical, or material support (i.e., reporting or organizing data, constructing databases): L. Xiang, J. Zhang, R. Hassan
Study supervision: I. Pastan

Acknowledgments

The authors thank David FitzGerald for helpful comments.

Grant Support

This research was supported by the Intramural Research Program of the NIH, NCI, Center for Cancer Research.

The costs of publication of this article were defrayed in part by the payment of page charges. This article must therefore be hereby marked *advertisement* in accordance with 18 U.S.C. Section 1734 solely to indicate this fact.

Received April 6, 2012; revised October 11, 2012; accepted October 28, 2012; published OnlineFirst November 6, 2012.

References

1. Kreitman RJ, Squires DR, Stetler-Stevenson M, Noel P, FitzGerald DJP, Wilson WH, et al. Phase I trial of recombinant immunotoxin RFB4 (dsFv)-PE38 (BL22) in patients with B-cell malignancies. J Clin Oncol 2005;23:6719–29.
2. Kreitman RJ, Stetler-Stevenson M, Margulies I, Noel P, FitzGerald DJP, Wilson WH, et al. Phase II trial of recombinant immunotoxin RFB4 (dsFv)-PE38 (BL22) in patients with hairy cell leukemia. J Clin Oncol 2009;27:2983–90.
3. Wayne AS, Kreitman RJ, Findley HW, Lew G, Delbrook C, Steinberg SM, et al. Anti-CD22 immunotoxin RFB4(dsFv)-PE38 (BL22) for CD22-positive hematologic malignancies of childhood: preclinical studies and phase I clinical trial. Clin Cancer Res 2010;16:1894–903.
4. Kreitman RJ, Tallman MS, Robak T, Coutre S, Wilson WH, Stetler-Stevenson M, et al. Phase I trial of anti-CD22 recombinant immunotoxin moxetumomab pasudotox (CAT-8015 or HA22) in patients with hairy cell leukemia. J Clin Oncol 2012;30:1822–8.
5. Hassan R, Bullock S, Premkumar A, Kreitman RJ, Kindler H, Willingham MC, et al. Phase I study of SS1P, a recombinant anti-mesothelin immunotoxin given as a bolus I.V. infusion to patients with mesothelin-expressing mesothelioma, ovarian, and pancreatic cancers. Clin Cancer Res 2007;13:5144–9.
6. Kreitman RJ, Hassan R, Fitzgerald DJ, Pastan I. Phase I trial of continuous infusion anti-mesothelin recombinant immunotoxin SS1P. Clin Cancer Res 2009;15:5274–9.

7. Hassan R, Sharon E, Schuler B, Mallory Y, Zhang J, Ling A, et al. Anti-tumor activity of SS1P with pemetrexed and cisplatin for newly diagnosed patients with advanced pleural mesothelioma and utility of serum mesothelin as a marker of tumor response [abstract]. In: Proceedings of the American Society of Clinical Oncology (ASCO) Annual Meeting Abstract; 2011 Jun 3–7; Chicago, IL.
8. Sampson JH, Akabani G, Archer GE, Berger MS, Coleman RE, Freidman AH, et al. Intracerebral infusion of an EGFR-targeted toxin in recurrent malignant brain tumors. Neuro Oncol 2008;10: 320–9.
9. Pai LH, Wittes R, Setser A, Willingham MC, Pastan I. Treatment of advanced solid tumors with immunotoxin LMB-1: an antibody linked to *Pseudomonas* exotoxin. Nat Med 1996;2:350–3.
10. Weldon JE, Pastan I. A guide to taming a toxin: recombinant immunotoxins constructed from *Pseudomonas* exotoxin A for the treatment of cancer. FEBS J 2011;278:4683–700.
11. Seetharam S, Chaudhary VK, FitzGerald D, Pastan I. Increased cytotoxic activity of *Pseudomonas* exotoxin and two chimeric toxins ending in KDEL. J Biol Chem 1991;266:17376–81.
12. Du X, Ho M, Pastan I. New immunotoxins targeting CD123, a stem cell antigen on acute myeloid leukemia cells. J Immunother 2007;30: 607–13.
13. Rozemuller H, Chowdhury PS, Pastan I, Kreitman RJ. Isolation of new anti-CD30 scFvs from DNA-immunized mice by phage display and biologic activity of recombinant immunotoxins produced by fusion with truncated *Pseudomonas* exotoxin. Int J Cancer 2001; 92:861–70.
14. Kreitman RJ, Pastan I. Importance of the glutamate residue of KDEL in increasing the cytotoxicity of *Pseudomonas* exotoxin derivatives and for increased binding to the KDEL receptor. Biochem J 1995;307(Pt 1):29–37.
15. Salvatore G, Beers R, Margulies I, Kreitman RJ, Pastan I. Improved cytotoxic activity toward cell lines and fresh leukemia cells of a mutant anti-CD22 immunotoxin obtained by antibody phage display. Clin Cancer Res 2002;8:995–1002.
16. Decker T, Oelsner M, Kreitman RJ, Salvatorae G, Wang QC, Pastan I, et al. Induction of caspase-dependent programmed cell death in B-cell chronic lymphocytic leukemia by anti-CD22 immunotoxins. Blood 2004;103:2718–26.
17. Johannes L, Decaudin D. Protein toxins: intracellular trafficking for targeted therapy. Gene Ther 2005;12:1360–8.
18. Fitzgerald D. Why toxins! Semin Cancer Biol 1996;7:87–95.
19. Weldon JE, Xiang L, Chertov O, Margulies I, Kreitman RJ, FitzGerald DJ, et al. A protease-resistant immunotoxin against CD22 with greatly increased activity against CLL and diminished animal toxicity. Blood 2009;113:3792–800.
20. Onda M, Nagata S, FitzGerald DJ, Beers R, Fisher RJ, Vincent JJ, et al. Characterization of the B cell epitopes associated with a truncated form of *Pseudomonas* exotoxin (PE38) used to make immunotoxins for the treatment of cancer patients. J Immunol 2006;177:8822–34.
21. Hansen JK, Weldon JE, Xiang L, Beers R, Onda M, Pastan I. A recombinant immunotoxin targeting CD22 with low immunogenicity, low nonspecific toxicity, and high antitumor activity in mice. J Immunother 2010;33:297–304.
22. Chang K, Pastan I. Molecular cloning of mesothelin, a differentiation antigen present on mesothelium, mesotheliomas, and ovarian cancers. Proc Natl Acad Sci U S A 1996;93:136–40.
23. Frierson HF Jr, Moskaluk CA, Powell SM, Zhang H, Cerilli LA, Stoler MH, et al. Large-scale molecular and tissue microarray analysis of mesothelin expression in common human carcinomas. Hum Pathol 2003;34:605–9.
24. O'Reilly MK, Tian H, Paulson JC. CD22 is a recycling receptor that can shuttle cargo between the cell surface and endosomal compartments of B cells. J Immunol 2011;186:1554–63.
25. Fujita M, Kinoshita T. GPI-anchor remodeling: potential functions of GPI-anchors in intracellular trafficking and membrane dynamics. Biochim Biophys Acta 2012;1821:1050–8.
26. Pastan I, Beers R, Bera TK. Recombinant immunotoxins in the treatment of cancer. Methods Mol Biol 2004;248:503–18.
27. Chowdhury PS, Viner JL, Beers R, Pastan I. Isolation of a high-affinity stable single-chain Fv specific for mesothelin from DNA-immunized mice by phage display and construction of a recombinant immunotoxin with anti-tumor activity. Proc Natl Acad Sci U S A 1998;95: 669–74.
28. Ho M, Hassan R, Zhang J, Wang QC, Onda M, Bera T, et al. Humoral immune response to mesothelin in mesothelioma and ovarian cancer patients. Clin Cancer Res 2005;11:3814–20.
29. Xiang X, Phung Y, Feng M, Nagashima K, Zhang J, Broaddus VC, et al. The development and characterization of a human mesothelioma *in vitro* 3D model to investigate immunotoxin therapy. PLoS ONE 2011;6: e14640.
30. Bang S, Nagata S, Onda M, Kreitman RJ, Pastan I. HA22 (R490A) is a recombinant immunotoxin with increased antitumor activity without an increase in animal toxicity. Clin Cancer Res 2005;11: 1545–50.
31. Siegall CB, Liggitt D, Chace D, Tepper MA, Fell HP. Prevention of immunotoxin-mediated vascular leak syndrome in rats with retention of antitumor activity. Proc Natl Acad Sci U S A 1994; 91:9514–8.
32. Onda M, Beers R, Xiang L, Lee B, Weldon JE, Kreitman RJ, et al. Recombinant immunotoxin against B-cell malignancies with no immunogenicity in mice by removal of B-cell epitopes. Proc Natl Acad Sci U S A 2011;108:5742–7.
33. Chowdhury PS, Pastan I. Improving antibody affinity by mimicking somatic hypermutation *in vitro*. Nat Biotechnol 1999;17: 568–72.
34. Reiter Y, Pastan I. Antibody engineering of recombinant Fv immunotoxin for improved targeting of cancer: disulfide-stabilized Fv immunotoxins. Clin Cancer Res 1996;2:245–52.
35. Wedekind JE, Trame CB, Dorywalska M, Koehl P, Raschke TM, McKee M, et al. Refined crystallographic structure of *Pseudomonas aeruginosa* exotoxin A and its implications for the molecular mechanism of toxicity. J Mol Biol 2001;314:823–37.
36. Thomas G. Furin at the cutting edge: from protein traffic to embryogenesis and disease. Nat Rev Mol Cell Biol 2002;3:753–66.
37. Morlon-Guyot J, Méré J, Bonhoure A, Beaumelle B. Processing of *Pseudomonas aeruginosa* exotoxin A is dispensable for cell intoxication. Infect Immun 2009;77:3090–9.
38. Ornatowski W, Poschet JF, Perkett E, Taylor-Cousar JL, Deretic V. Elevated furin levels in human cystic fibrosis cells result in hypersusceptibility to exotoxin A-induced cytotoxicity. J Clin Invest 2007;117: 3489–97.
39. Chiron MF, Fryling CM, FitzGerald D. Furin-mediated cleavage of *Pseudomonas* exotoxin-derived chimeric toxins. J Biol Chem 1997;272:31707–11.
40. Moehring JM, Inocencio NM, Roertson BJ, Moehring TJ. Expression of mouse furin in a Chinese hamster cell resistant to *Pseudomonas* exotoxin A and viruses complements the genetic lesion. J Biol Chem 1993;18:2590–4.
41. Onda M, Willingham M, Wang QC, Kreitman RJ, Tsutsumi Y, Nagata S, et al. Inhibition of TNF-alpha produced by Kupffer cells protects against the nonspecific liver toxicity of immunotoxin anti-Tac(Fv)-PE38, LMB-2. J Immunol 2000;165:7150–6.
42. Druey KM, Greipp PR. Narrative review: the systemic capillary leak syndrome. Ann Intern Med 2010;153:90–8.
43. Baluna R, Rizo J, Gordon BE, Ghetie V, Vitetta ES. Evidence for a structural motif in toxins and interleukin-2 that may be responsible for binding to endothelial cells and initiating vascular leak syndrome. Proc Natl Acad Sci U S A 1999;96:3957–62.
44. Siegall CB, Liggitt D, Chace D, Mixan B, Sugai J, Davidson T, et al. Characterization of vascular leak syndrome induced by the toxin component of *Pseudomonas* exotoxin-based immunotoxins and its potential inhibition with nonsteroidal anti-inflammatory drugs. Clin Cancer Res 1997;3:339–45.
45. Brenner BM, Hostetter TH, Humes HD. Glomerular permselectivity: barrier function based on discrimination of molecular size and charge. Am J Physiol 1978;234:F455–60.
46. Kreitman RJ, Pastan I. Accumulation of a recombinant immunotoxin in a tumor *in vivo*: fewer than 1000 molecules per cell

are sufficient for complete responses. Cancer Res 1998;58: 968–75.
47. Traini R, Kreitman RJ. Renal excretion of recombinant immunotoxins containing *Pseudomonas* exotoxin. Bioconjug Chem 2011;22:736–40.
48. Boron WF, Boulpaep EF, editors. Medical physiology: a cellular and molecular approach. 2nd ed. Philadelphia, PA: Elsevier/Saunders; 2009.
49. Bera TK, Pastan I. Comparison of recombinant immunotoxins against LeY antigen expressing tumor cells: influence of affinity, size, and stability. Bioconjug Chem 1998;9:736–43.
50. Zhang Y, Hansen JK, Xiang L, Kawa S, Onda M, Ho M, et al. A flow cytometry method to quantitate internalized immunotoxins shows that taxol synergistically increases cellular immunotoxins uptake. Cancer Res 2010;70:1082–9.